Magnetoelectric coupling on fused azulene oligomers

A. Valentim,[1,2,3,*] D. J. García,[3,4,†] and J. A. Plascak[1,2,5,‡]

[1]*Departamento de Física, Instituto de Ciências Exatas, Universidade Federal de Minas Gerais, Caixa Postal 702, 30123-970 Belo Horizonte, Minas Gerais, Brazil*

[2]*Departamento de Física, Universidade Federal da Paraíba, Caixa Postal 5008, 58051-900 João Pessoa, Paraíba, Brazil*

[3]*Consejo Nacional de Investigaciones Científicas y Técnicas (CONICET), Argentina*

[4]*Centro Atómico Bariloche and Instituto Balseiro, CNEA, 8400 Bariloche, Argentina*

[5]*University of Georgia, Department of Physics and Astronomy, Athens, Georgia 30602, USA*

(Received 24 April 2021; revised 22 February 2022; accepted 10 May 2022; published 24 May 2022)

The global magnetic phase diagram for fused azulene oligomers is obtained by using a fermionic Hubbard model, which is an intermediate between the molecular Pariser-Parr-Pople empiric Hamiltonian and the spin-1/2 antiferromagnetic Heisenberg model. We employ the density matrix renormalization group (DMRG) approach to explore the ground state properties of azulene-like molecules as a function of the electronic correlation and the oligomer size. It is shown that, depending on the length of the oligomer, fused azulene transitions from a singlet ($S = 0$) to a higher-spin ($S = 1, 2$) ground state. Near the quantum magnetic phase transition the electric dipole moment, present on fused azulene molecules, couples with the magnetic moment leading to a divergent magnetoelectric susceptibility at the boundary lines of the magnetic phase diagram. These spontaneous electric and magnetic polarizations, together with the magnetoelectric coupling between them, indeed corroborate that these fused azulene oligomers can be viewed as a purely organic multiferroic material, being a magnetoelectric molecule.

DOI: 10.1103/PhysRevB.105.174426

I. INTRODUCTION

The name multiferroic is usually used to address a class of materials which simultaneously display more than one order parameter. The physical properties of these systems can be controlled by an external agent (like external fields or tensions, for example) and, more interestingly, a coupling between the order parameters can take place for some of these single-compound materials (also referred to as single-phase materials). Magnetoelectric multiferroics, for instance, exhibit at least one kind of magnetic ordering with magnetization (**M**) along with electric polarization (**P**). In some of these rare single-phase multiferroics, the moments **M** and **P** may be modified by either electric (**E**) or magnetic (**H**) external fields. The coexistence of the two forms of ordering (nonzero macroscopic magnetic and electric dipole moments) leads to additional interactions, allowing for induction of magnetization by **E** or charge polarization by **H**. This magnetoelectric coupling opens the possibility for charge and spin control by either of these conjugated fields. For a short review on multiferroics see, for instance, Refs. [1,2].

Recent advances in understanding the microscopic origins of the magnetoelectric (ME) effect on single-phase materials, including metal-organic compounds [3–5], have shown that promising candidates for controlled ME switchings are compounds with electronic states close to the ground state [6,7]. In these materials, the electronic states close to the ground state are energetically lowered by magnetoelectric contributions under a perturbation such as an external field. Consequently, frustrated systems, or systems in the vicinity of phase boundaries, as well as quantum critical points, are prime candidates for magnetic phase control using **E** or, indirectly, electric polarization by using **H**. In this way, fused azulene molecules (forming a quasi-one-dimensional system and whose geometries do not have inversion symmetry) exhibit the above mentioned characteristics and have already been theoretically predicted to be a possible purely organic multiferroic candidate [8].

Molecular organic electronic devices made of oligo-acene, consisting of even-ring molecules made of fused benzene in the acene conformation, are already a reality [9–12]. Similar quasi-one-dimensional geometries, explored by different computational approaches, have also pointed to the existence of magnetism at ground state when odd-rings are present in these theoretical heterostructures [13–15]. Some of these molecules can also support electric polarization, making available a large set of possible magnetoelectric molecules. These are long molecules with seven or more rings. Nevertheless, it has been recently reported from experiments that the stability of oligo-acenes increased upon the introduction of azulene molecules into fused benzene oligomers [16].

Benzene and azulene oligomers are planar structures made of only carbon (C) and hydrogen (H) atoms. Within the Hückel molecular orbital theory [17] the physics of these conjugated systems can be understood in terms of an extended

*valentim@fisica.ufmg.br
†garciad@cab.cnea.gov.ar
‡pla@uga.edu

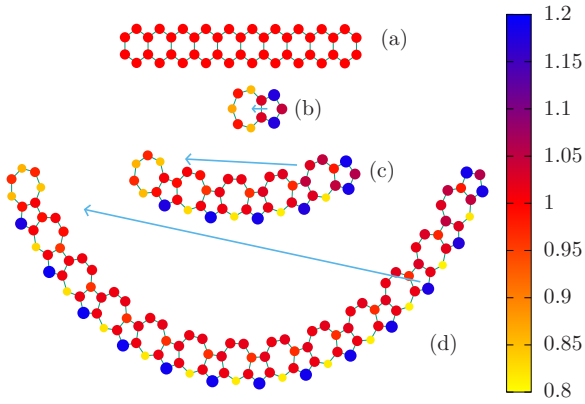

FIG. 1. (a) Skeleton structure for 10-benzene, (b) a single azulene molecule, and (c) and (d) 5- and 13-azulene oligomers, respectively. The area of the dots, as well as the color gradient on the right, is proportional to the electronic charge when the Coulomb interaction between electrons at the same site is not taken in account. The arrows represent the electric polarization due to the unbalanced charge distribution through n-azulene molecules. The hydrogen atoms and the corresponding bonds are not shown in this figure for the sake of clarity.

molecular orbital with a p_z orbital for each carbon atom. At half-filled band the electronic distribution of charge on π orbitals allows kinetic and magnetic frustration on azulene-like geometries, which are absent on benzene, due to the rings with odd number of carbon atoms. For this reason, and because of the lack of inversion symmetry, the azulene molecule displays spontaneous charge polarization and we would expect it to have a lower-energy triplet excitation than benzene molecules. The fused-benzene series of molecules has already been synthesized up to nine monomers [18,19] and it has been found not to display either charge or magnetic polarization.

As a matter of example, Fig. 1 illustrates the skeleton geometries for (a) a 10-acene oligomer (5-fused benzene), (b) a single azulene molecule, (c) a 5-fused azulene oligomer, and (d) a 13-fused azulene oligomer. The dots illustrate the carbon atoms' positions along with the charge distribution and electric dipole moment computed using a tight-binding approach [20]. Although the tight-binding charge distributions, depicted by the dots in Fig. 1, seem more or less the same on each site, the electric dipole moment (arrow) evinces that the five-membered ring, as shown in (b), does accumulate more negative charge relative to the seven-membered ring. To the best of our knowledge, there exist geometry optimizations based on density functional theory (DFT) for the azulene molecule configurations shown in Fig. 1 up to 6-fused azulene [21]. There are also independent geometry optimizations of shorter linear molecules made of fused azulene and benzene [14–16]. From the above four different studies [14–16,21], the planar geometry of these polycyclic aromatic hydrocarbon systems is confirmed and almost negligible bond length variations are obtained. Thus, to compute the electric polarization, one can consider perfect 5 and 7 carbon rings.

These fused azulene configurations have been theoretically studied using different computational techniques [8,15,21,22]. DFT and effective valence bond explorations show the presence of a nonferromagnetic to ferromagnetic transition when 6 or more azulene molecules are fused together [21]. A subsequent study using density matrix renormalization group (DMRG) reports a ferromagnetic transition for a shorter azulene oligomer (5-fused azulene molecules), together with a charge polarization. These results suggest that the fused azulene oligomers could be indeed a multiferroic molecule [8]. A configurational interaction study for shorter oligomers (2- and 3-fused azulene) conjectures that the spin frustration, due to the geometry of the azulene molecule, could be the origin of the magnetic polarization in longer odd-membered chains [22].

Other studies [14,15,23] have shown different magnetic molecules with configurations not given by Ovchinnikov's rule [24]. Despite that the polycyclic aromatic hydrocarbon molecules found in these simulations have the potential to be molecular magnets, only the fused azulene with geometry such as in Fig. 1(c) and those in Refs. [8,15,21,22] have already been suggested as possible, and unique so far, purely organic multiferroics.

The fused azulene geometry has also been explored by using the spin-1/2 antiferromagnetic Heisenberg Hamiltonian [8] and the fermionic Hubbard Hamiltonian [15]. For both models the magnetic ground state moment has been observed to increase with the number of monomers. In addition, many interesting features have also been reported, such as a reentrant nonmagnetic state when the exchange interaction strength of the common bond between rings is varied [13]. Although the origin of the magnetism in fused azulene molecules is not yet completely understood, their geometries seem in fact to show a route to synthesize purely organic magnetoelectric molecules.

An appropriate description of the magnetic excitations in these conjugated systems demands that full electron correlations should be taken into account. However, such a many-body problem imposes a severe restriction on the size of the system to be explored either analytically or computationally. Even approximate Hamiltonians, like the phenomenological Pariser-Parr-Pople (PPP) Hamiltonian [25,26], which considers full long-range Coulomb interactions, are very difficult to be solved for large systems. Although graphene nanoribbons with 100 carbon atoms have already been studied within the PPP model using DMRG algorithms [27,28], Hamiltonians such as the Heisenberg [8,13,14], Hubbard, and its variations such as effective Hubbard or extended Hubard models [15,29,30] have also been used to address such systems. In a previous work [15], it has been shown that Hubbard and PPP models, also DFT, give similar results for the electronic and spin ground state configuration. Moreover, it has been reported in Ref. [29] that an effective Hubbard model can be obtained from extended Hubbard models (like PPP) that describe well the charge and spin state. Similarly, the Supplemental Material of Ref. [21] also uses the Hubbard model to obtain the spin configuration on azulene molecules. These works show that the Hubbard Hamiltonian could be well suited for studying the main transition properties of the present azulene molecules.

The Hubbard Hamiltonian, which we will use in this work, neglects the Coulomb repulsion between electrons of different atoms and takes into account just the interaction between

electrons at the same site (on-site Coulomb repulsion). This model simplifies the complexity of the problem while retaining electronic correlations and has been successfully used to elicit information on correlated systems, including conjugated molecules (see, for instance, Refs. [31–33]).

When long-range Coulomb interactions are neglected, the important parameter is naturally the effective strength of the on-site Coulomb interaction (an interesting discussion on this subject for graphene and graphite can be found in Ref. [34]). The evolution of the electronic structure with the increase of the on-site interaction has also been investigated in nonorganic multiferroics like the Bi_2FeCrO_6 perovskite and parent structures [35].

In the present work, we employ the density matrix renormalization group (DMRG) approach and the Hubbard Hamiltonian to explore the ground state properties of azulene-like molecules as a function of the electronic correlation and the oligomer size. Thus, we obtain the global magnetic phase diagram for these molecules in the plane of the oligomer length n (for $1 \leqslant n \leqslant 17$) versus the ratio of the on-site Coulomb interaction to the hopping constant between nearest-neighbor carbon atoms. In addition, we take a step forward, by showing that there is a coupling between the magnetic and charge polarization, leading to a divergent magnetoelectric susceptibility near the magnetic phase transition. This last result indicates that fused azulene molecules could in fact be considered a purely organic magnetoelectric multiferroic.

The plan of the paper is the following. In the next section we briefly describe the Hubbard model for the n-fused azulene oligomers and give some details of the DMRG numerical approach. Section III conveys the results for $n = 1$-, 5-, and 13-azulene fused oligomers and the global magnetic phase diagram in the plane of the oligomer length versus the ratio of the on-site Coulomb interaction to the hopping constant. Some concluding remarks are given in the last section.

II. MODEL AND METHOD

A. Model

We employ herein the Hubbard model [36] to describe the electronic interactions present in conjugated systems of the kind depicted in Fig. 2. The model Hamiltonian $\hat{H}$ basically contains a noninteracting part $\hat{H}_0$ and a term $\hat{H}_1$ that incorporates the on-site electron-electron interaction, namely

$$\hat{H} = \hat{H}_0 + \hat{H}_1. \tag{1}$$

The noninteracting part is a tight-binding-like Hamiltonian

$$\hat{H}_0 = -t \sum_{\langle i,j\rangle;\sigma} (\hat{c}^\dagger_{i\sigma}\hat{c}_{j\sigma} + \hat{c}^\dagger_{j\sigma}\hat{c}_{i\sigma}), \tag{2}$$

which describes the kinetic energy with a hopping constant t between nearest-neighbor p_z orbitals of carbon atoms (henceforth, we will take t as the energy unit). In this framework, the operator $\hat{c}^\dagger_{i\sigma}$ ($\hat{c}_{i\sigma}$) creates (annihilates) an electron of spin σ, localized at site i. $\langle i, j\rangle$ indicates a sum over nearest neighbors.

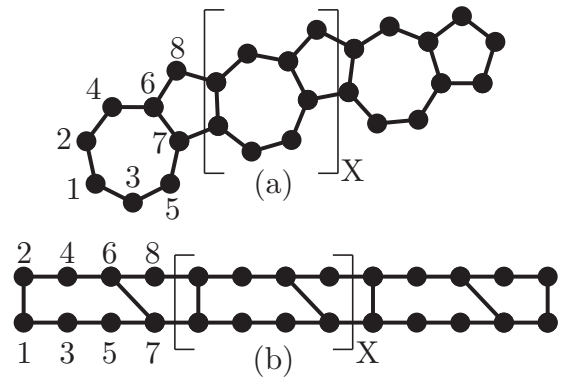

FIG. 2. (a) Part of a fused azulene structure and (b) the corresponding DMRG ladder-like scheme for building fused azulenes. The [ ]X portion is the building block of the oligomer. The numbers label, for the first eight sites of the building block of the oligomer, the carbon atoms on the original molecule geometry, panel (a), and on the corresponding ladder structure, panel (b). In the latter, the numbers show the order of sites as implemented in our DMRG algorithm.

The interacting part of $\hat{H}$ can be written in the form

$$\hat{H}_1 = U \sum_{i=1}^{N} \left(\hat{n}_{i\uparrow} - \frac{1}{2}\right)\left(\hat{n}_{i\downarrow} - \frac{1}{2}\right), \tag{3}$$

where U is the magnitude of the on-site Coulomb interaction. The total electron density is $\hat{n}_i = \hat{n}_{i\uparrow} + \hat{n}_{i\downarrow}$, with $\hat{n}_{i\sigma} = \hat{c}^\dagger_{i\sigma}\hat{c}_{i\sigma}$ being the local particle number operator for electrons of spin σ at site i. N denotes the total number of sites (carbon atoms), which is equal to the number of electrons in the system. At half-filled band, the factor $1/2$ fixes the chemical potential for mean occupation $\langle \hat{n}_i \rangle = 1$ on each site.

At this point it is worthwhile to address some comments on the parameters of this Hamiltonian. It is indeed unclear how to devise a way to change U for the p orbital of the carbon atom. However, it has been shown for graphene and benzene that optimal values of U/t differ for each compound [29]. In this reference, it has also been shown that the effective on-site Coulomb repulsion U of the Hubbard model can result from an extended Hubbard model (PPP) as a competition between the local part of the interaction and a weighted average of nonlocal interactions. The infinite limit $U/t \to \infty$ of the Hubbard model (Heisenberg model) has been used to find possible magnetic molecules [14], as well as perturbations around $U/t \sim 0$ [15]. C_{20} molecules, with different geometries, have also been studied by using the Hubbard model with different numerical techniques [30]. In this work different estimates of the U to t ratio for the three C_{20} isomers have been reported.

It is quite clear from the above discussion that the U/t value is not well defined for different compounds and can be even modified by the environment and geometry where the molecule is placed. In this sense, every model adds in the understanding of the magnetic and electronic properties of such molecules. For this reason, in this work we try to give a full picture, in the case of a Hubbard model, of the possible phases as a function of the ratio U/t.

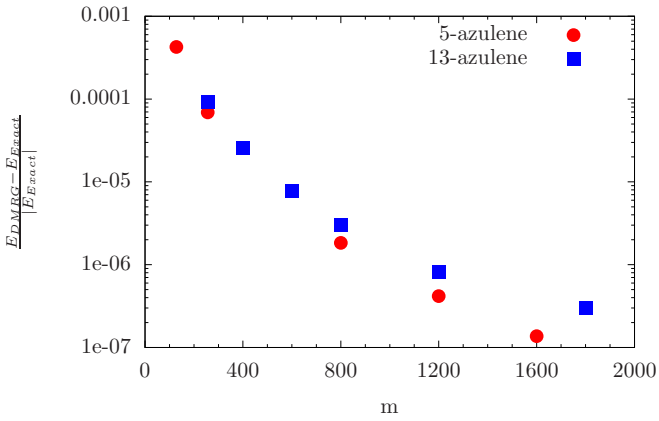

FIG. 3. Difference of the ground state energies for the 5-azulene and 13-azulene as a function of the number of kept states m. E_{DMRG} stands for the ground state energy of the Hubbard model with $U = 0$ computed at $S_z = 0$ spin subspace by using DMRG. E_{exact} stands for the exact matrix diagonalization of the Hamiltonian at the same conditions.

B. Density matrix renormalization group

Although the DMRG algorithm was first designed to study one-dimensional problems [37], different low-dimensional structures, like quasi-one-dimensional models, can also be accurately treated within this approach [15,38,39]. One simple example is a two-legged ladder structure, which is quite suitable for representations of oligo-acenes [as in Fig. 1(a)] and fused azulenes [as in Figs. 1(c) and 1(d)] as well. As shown in Fig. 2, one can easily map any n-fused azulene to the Hubbard Hamiltonian with hopping defined on a two-legged ladder with alternating perpendicular and skewed rungs. It turns out that such finite strip structure can be easily implemented on a DMRG algorithm.

It is clear that oligomers described by the Hamiltonian in Eq. (1) have SU(2) symmetry, so we can take advantage of the degeneracy of spin projections M_S for a total spin S, and compute the low-lying energy of the system in a chosen subspace. The ground state energy in the S subspace is found when $|M_S| \leqslant S$ and $E(M_S) \leqslant E(M_S + 1)$, where $E(M_S)$ is the lowest energy within M_S subspace [40,41]. In this case, the DMRG algorithm computes the total energy with a fixed number of electrons (equal to the number of carbon atoms) and fixed total spin projection M_S.

In order to establish the accuracy of our DMRG simulations we have compared the DMRG results for the energy at $U = 0$ with the exact solution of the tight-binding Hamiltonian $\hat{H}_0$. We have obtained the ground state (GS) energy with different sizes of the Hilbert space, keeping a typical cutoff in the number of dominant density matrix eigenvectors $m = 800$ to a maximum of $m = 1800$ states per block at the final iteration. In these conditions the energy precision is in the fourth decimal digit. The relative energy error is comparable to the DMRG weight lost, and is kept lower than 10^{-5} in the worst cases. In Fig. 3 we a have a numerical comparison, at $U = 0$, of the relative difference of the ground state energies computed from the exact matrix diagonalization E_{exact} and those coming from the DMRG procedure E_{DMRG} for different values of m and for 5- and 13-azulene oligomers. Note that E_{exact} is negative and, due to the variational character of the DMRG, E_{DMRG} is always greater than E_{exact}.

III. RESULTS AND DISCUSSION

We have performed DMRG simulations to compute the spin gap excitations of the energy, the charge polarization, and the electric susceptibility for n-fused azulene oligomers for $1 \leqslant n \leqslant 17$; see Figs. 1(b) and 1(c) for examples with $n = 1, 5$, and 13. These specific conjugated configurations, with an armchair edge in one side of the chain and zigzag edges on the other side of the chain (in analogy with graphene edges), lead to a kind of semicircular shape when 17 azulene molecules are fused together (138 carbon atoms).

The spin gap excitations of the energy is defined as the difference between the energy of the higher spin configuration $E(M_S)$, computed at the higher M_S subspace, and the energy of the spin configuration $E(M_S - 1)$, namely

$$\Delta_{M_S} = E(M_S) - E(M_S - 1), \tag{4}$$

for $M_S = 1, 2, \ldots$.

The vector charge polarization, computed at a given value of the M_S subspace, is defined by the spontaneous electric dipole moment

$$\mathbf{P}(M_S) = \sum_i (\langle n_i \rangle - 1)\mathbf{r}_i, \tag{5}$$

where $\langle n_i \rangle$ is the average on-site electronic charge at the subspace M_S and the number 1 here arises due to the nucleus charge.

Finally, the magnetoelectric charge susceptibility is given by

$$\chi_P = \frac{P(M_S) - P(M_S - 1)}{E(M_S) - E(M_S - 1)}, \tag{6}$$

where $P(M_S)$ is the magnitude of the vector charge polarization $\mathbf{P}(M_S)$.

A. Single azulene molecule ($n = 1$ and 10 carbon atoms)

We start by showing the magnetic and electric ground state (GS) properties for a single azulene-like molecule, Fig. 1(b), as the ratio U/t is varied. In Fig. 4 we have the corresponding results as a function of U/t ranging from zero (uncorrelated system) up to $U/t = 10$ (strongly correlated system). Figure 4(a) shows the difference of the energy computed on the $M_S = 1$ and $M_S = 0$ spin subspaces. A finite spin gap indicates that only a singlet ground state is found for this molecule, in agreement with previous results from Refs. [8,21,22]. A nonvanishing singlet-triplet spin gap for the azulene molecule with U/t shows that the azulene molecule does not undergo any magnetic phase transition and remains always in a singlet $S = 0$ state.

Figure 4(b) shows the magnitude of the vector charge polarization computed at $M_S = 0$ and $M_S = 1$ subspaces. In both cases, the computed electric dipole moment strongly decreases when the system goes from the weak electronically correlated to the correlated regime. This behavior reflects the strong on-site correlation that leads the electrons to avoid the

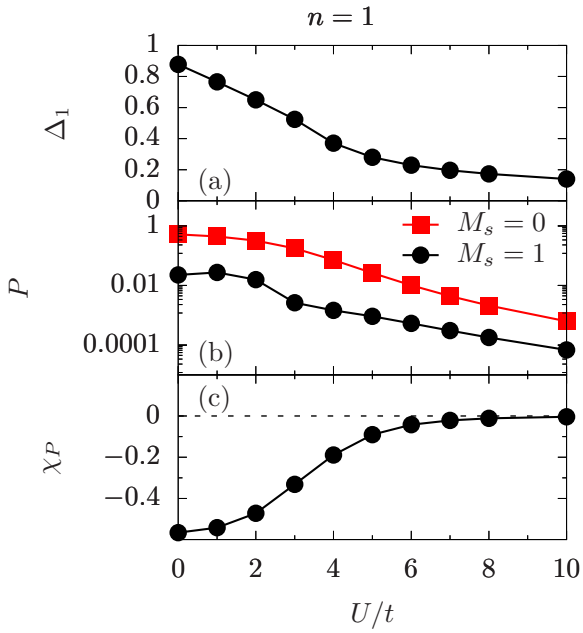

FIG. 4. (a) The singlet-triplet spin gap Δ_1; (b) absolute value of the electric polarization P, in logarithmic scale; and (c) susceptibility χ_P, all of them as a function of U/t for the single azulene molecule in Fig. 1(b) (10 carbon atoms). The dashed line shows the asymptotic limit of the susceptibility for large values of U/t and full lines are just guides to the eyes. The DMRG data have an error bar which is smaller than the symbol sizes.

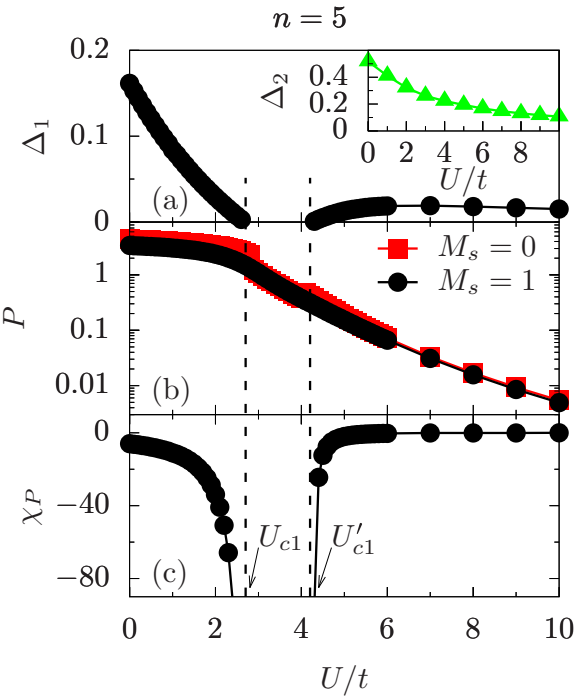

FIG. 5. The same as Fig. 4 for the 5-azulene oligomer, in this case with a total of 42 carbon atoms. The inset in (a) shows Δ_2, which is the difference of the energy computed on the $M_S = 2$ and $M_S = 1$ spin subspaces. U_{c1} is the critical value of the on-site Coulomb interaction at the transition from the $M_S = 0$ to the $M_S = 1$ spin subspaces and U'_{c1} is the corresponding critical interaction at the transition from the $M_S = 1$ back to the $M_S = 0$ spin subspaces. As before, the DMRG data have error bars which are smaller than the symbol sizes.

double occupancy on each carbon atom, thus favoring localization and diminishing the value of the charge polarization. As a consequence, the magnetoelectric charge susceptibility increases (from its negative saturation value) with U/t, and goes to zero in the strong correlated regime region, as shown in Fig. 4(c).

B. Five-fused azulene molecule ($n = 5$ and 42 carbon atoms)

The same analysis for a five-fused azulene-like molecule is displayed in Fig. 5. One can clearly see that for this oligomer length, a spontaneous phase transition from the singlet ($S = 0$) to the triplet ($S = 1$) ground state occurs at $U_{c1}/t \cong 2.6$, as shown in Fig. 5(a). Here, U_{c1} is the critical value of the electronic correlation in which the system undergoes a phase transition. Furthermore, another transition from the triplet back to the singlet ground state is also observed for $U'_{c1}/t \cong 4.3$. The inset in Fig. 5(a) shows the energy difference Δ_2 of the system at $M_S = 2$ and $M_S = 1$ subspaces. The finite spin gap $\Delta_2 > 0$ in the entire range of U/t indicates that the ground state of the system belongs indeed only to the subspaces with $S = 0$ and $S = 1$, and no transition to higher values of the total spin is present.

The multiferroic character of the system is revealed by the abrupt change of the electric polarization and magnetoelectric susceptibility that occurs near the magnetic phase transition. Figure 5(b) shows the charge polarization magnitude computed at $M_S = 0$ and $M_S = 1$ total spin subspaces. We observe that the charge polarization at $M_S = 0$ subspace is larger in the singlet ground state than in the $M_S = 1$ subspace for $U/t < U_{c1}/t$ and $U/t > U'_{c1}/t$. The polarization is the same between U_{c1}/t and U'_{c1}/t (similar behavior happens for the PPP model [8]). At the borders we have a sudden change in the dipole moment when the spin GS goes from the singlet to triplet phases, and vice versa. This change at the absolute value of polarization leads to a strong magnetoelectric response near the magnetic transition, as indicated by the divergence of the charge susceptibility around U_{c1}/t and U'_{c1}/t, as shown in Fig. 5(c). This means that the charge polarization can be tuned by changing the external magnetic field value around the quantum magnetic phase transition.

It should be stressed that the values of U_{c1}/t and U'_{c1}/t have been obtained from the spin energy gap and, besides the intrinsic errors from the DMRG calculations, they also carry uncertainties from the steps of U/t used in the simulations. Taking into account all these uncertainties we were able to locate these transition values with error of the order ± 0.1 and ± 0.5 (for short and long oligomer sizes, respectively). For the present oligomer length the critical values are $U_{c1}/t = 2.6 \pm 0.1$ and $U'_{c1}/t = 4.3 \pm 0.1$.

C. 13-fused azulene molecule ($n = 13$ and 106 carbon atoms)

The results for the 13-fused azulene molecule are depicted in Fig. 6. It is interesting to see now that besides a transition from the singlet to the triplet ground state around $U_{c1}/t \cong 0.7$,

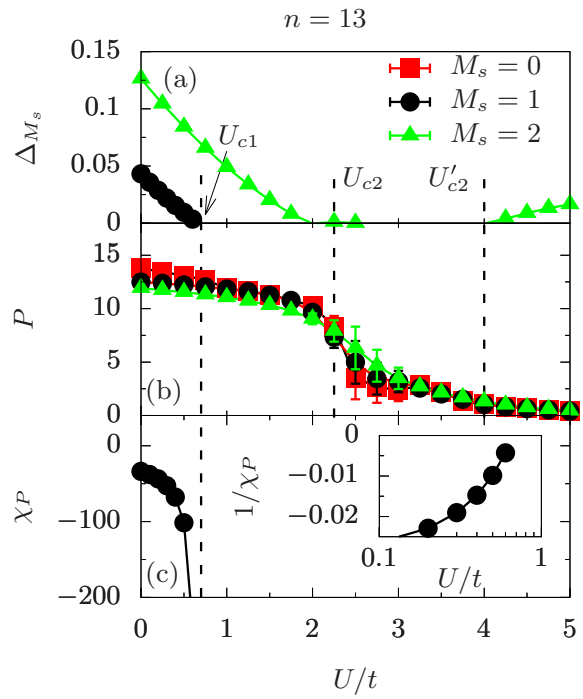

FIG. 6. (a) Spin energy gap Δ_{M_S}; (b) absolute value of the electric polarization P; and (c) susceptibility χ_P (the inset shows the corresponding inverse of χ_P). All quantities are given as a function of U/t for the 13-azulene oligomer with 106 carbon atoms for three different values of the total spin $M_S = 0, 1, 2$. The DMRG data have error bars which are smaller than the symbol sizes for most U/t values. Notably, for $2 \lesssim U/t \lesssim 3$ the polarization shows a large uncertainty.

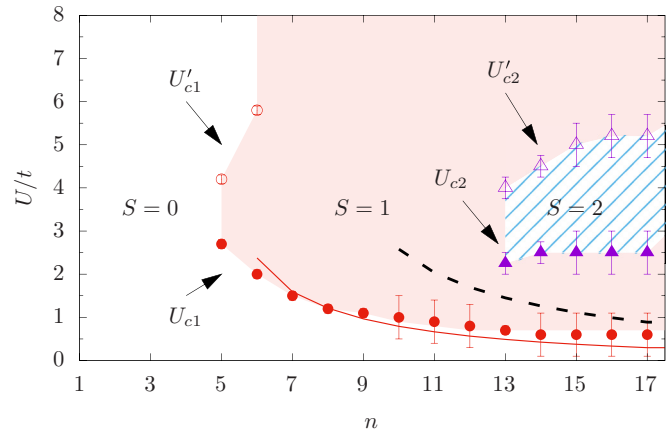

FIG. 7. Ground state magnetic phase diagram in the n versus U/t plane. The empty, shaded, and hatched regions represent, respectively, the ground state phases of the total spin $S = 0$, $S = 1$, and $S = 2$ of the molecule. The symbols represent the quantum phase transitions between different total spin of the molecule, with full symbols to a higher spin value and open symbols back to the lower spin value. The lines are second-order perturbation theory calculations [15] for the closing value of the spin gap at spin $S = 0$ to $S = 1$ transition (Δ_1; full line) and $S = 1$ to $S = 2$ spin ground state (Δ_2; dashed line) transition, respectively.

an additional transition to the $S = 2$ ground state takes place around $U_{c2}/t \cong 2$. The $S = 2$ ground state, however, is not stable for larger values of the electron-electron repulsion and for $U'_{c2}/t \cong 4$ the system transitions back to the $S = 1$ state.

These quantum phase transitions are clearly seen in the spin gap energy Δ_{M_S} shown in Fig. 6(a), namely Δ_1 between the states $M_S = 1$ and $M_S = 0$ and Δ_2 between the states $M_S = 2$ and $M_S = 1$. We have noticed that this triple transition behavior occurs here only for lengths $n \geqslant 13$, while using the PPP model such transitions are predicted to happen when the system reaches about 11 fused azulene units [8]. Note that at this point we are introducing a convenient notation U_{c1}/t and U_{c2}/t for transitions to the spin states $S = 1$ and $S = 2$, respectively, and the primed quantities U'_{c1}/t and U'_{c2}/t for transitions back to the spin states $S = 0$ and $S = 1$.

The magnitude of the charge polarization computed at the $M_S = 0$, $M_S = 1$, and $M_S = 2$ subspaces is shown in Fig. 6(b). As happens for the 5-fused azulene, the dipole moment abruptly varies when the spin of the GS goes from singlet to higher spin GS ($S = 1, 2$). Again, this behavior of the absolute value of the polarization causes a divergence of χ_P near the magnetic transition, as shown in Fig. 6(c). The inset in Fig. 6(c) depicts the inverse of the susceptibility as a function of U/t. For this oligomer size, however, the electric polarization for different values of M_S and $2 \lesssim U_c/t \lesssim 3$ presents a large uncertainty. For this reason we have estimated the transition point by using only the energy gap Δ_{M_S} for all oligomer sizes.

Taking into account all the error sources we can estimate, for this oligomer size, $U_{c1}/t = 0.7 \pm 0.1$, $U_{c2}/t = 2.25 \pm 0.25$, and $U'_{c2}/t = 4.0 \pm 0.25$.

D. Quantum magnetic phase diagram

Following the above procedure in the same way for other oligomer lengths, we can construct the magnetic ground state phase diagram for these azulene-like molecules by computing the critical value of the ratio U_c/t at each transition as a function of the oligomer size n. In Fig. 7, for any oligomer length $n \leqslant 17$, U_c gives the corresponding critical value of the electronic correlation for which the system undergoes a quantum phase transition. S is the corresponding value of the ground state spin. As previously done, for each oligomer size n, the strengths of the ratios U_{ci}/t and U'_{ci}/t, $i = 1, 2$, have been estimated with a precision of at least 0.5.

It is clear from Fig. 7 that depending on the molecule length, the system (i) stays in the singlet state for any value of the on-site Coulomb interaction for $n < 5$; (ii) for $5 \leqslant n \leqslant 6$ it displays a quantum transition from the singlet ($S = 0$) to the triplet ($S = 1$) ground state at U_{c1}/t and back again to the singlet state at U'_{c1}/t; (iii) in the region $6 < n < 13$ only a quantum transition from the singlet to the triplet ground state is observed; and (iv) after the transition from the singlet to the triplet state, it can additionally transition to the quintuplet $S = 2$ ground state at U_{c2}/t, and back again to the triplet state at U'_{c2}/t, when $13 \leqslant n \leqslant 17$. In short, the molecules become ferromagnetic as soon as their length is greater than $n = 5$. The results are summarized in Table I, together with critical values obtained from a second-order perturbation approach for comparison.

TABLE I. Critical values of the U/t ratio for each oligomer size n obtained by using the DMRG. U_{c1}/t is the transition interaction from the singlet ($S=0$) to the triplet ($S=1$) spin state. U'_{c1}/t is the transition interaction from the triplet ($S=1$) back to the singlet ($S=0$) spin state. Similarly, U_{c2}/t is from the triplet ($S=1$) to the quintuplet ($S=2$) spin state with U'_{c2}/t from the quintuplet ($S=2$) back to the triplet ($S=1$) spin state. U^{PT}_{c1}/t and U^{PT}_{c2}/t are, respectively, the critical interaction values for the singlet ($S=0$) to the triplet ($S=1$) and for the triplet ($S=1$) to the quintuplet ($S=2$) spin states according to a second-order perturbation theory [15].

n-azulene	U_{c1}/t	U'_{c1}/t	U_{c2}/t	U'_{c2}/t	U^{PT}_{c1}/t	U^{PT}_{c2}/t
5	2.7 ± 0.1	4.2 ± 0.1				
6	2.0 ± 0.1	5.8 ± 0.1			2.376	
7	1.5 ± 0.1				1.593	
8	1.2 ± 0.1				1.211	
9	1.1 ± 0.1				0.965	
10	1.0 ± 0.5				0.792	2.578
11	0.9 ± 0.5				0.664	2.037
12	0.8 ± 0.5				0.566	1.697
13	0.7 ± 0.1		2.25 ± 0.25	4.0 ± 0.25	0.488	1.452
14	0.7 ± 0.5		2.5 ± 0.25	4.5 ± 0.25	0.426	1.263
15	0.7 ± 0.5		2.5 ± 0.5	5.0 ± 0.5	0.375	1.113
16	0.7 ± 0.5		2.5 ± 0.5	5.2 ± 0.5	0.333	0.990
17	0.7 ± 0.5		2.5 ± 0.5	5.2 ± 0.5	0.298	0.888

IV. CONCLUDING REMARKS

The global magnetic phase diagram depicted in Fig. 7 shows indeed an interesting pattern of reentrant magnetic phases. Unfortunately, up to our knowledge, we still do not have in the literature, for the present model, any similar phase diagram to compare with. However, some particular details of the behavior shown in Fig. 7 can be correlated with results from other analogous systems. For instance, similar reentrances have also been observed when using the Hubbard model to explore different quasi-one-dimensional geometries, such as quantum nanowires of As/Si(100) [42] and generalizations of the quantum J_1-J_2 model defined on two-legged ladders with skewed rungs [13].

In Ref. [8] were computed the singlet and the triplet spin ground states using a semiempirical approach, namely the PPP model with the intersite Coulomb interaction parametrized by the Ohno formula [43] and fixed on-site Coulomb interaction $U/t = 4.7$. In this case, the transition happens when six azulene molecules are fused. Note that within the present fermionic approach the transition only occurs when the oligomer length reach five fused molecules. This is in fact an expected result because the Hubbard model plays a role between a finite fixed value for the Coulomb interaction (PPP Hamiltonian) and infinite intersite Coulomb repulsion (Heisenberg Hamiltonian).

We note that the U/t strength needed to induce the ferromagnetic phase for $n \geqslant 5$ decreases when increasing the oligomer size (it eventually saturates for $n \geqslant 13$), in qualitative agreement with results from a simple second-order perturbation treatment of electronic correlations by means of Rayleigh-Schrödinger perturbation theory analysis [15]. Thus, besides presenting the full n versus U/t phase diagram for fused-azulenes, the present work shows that a divergent magnetoelectric susceptibility appears close to the magnetic transition, signalizing a magnetoelectric multiferroic behavior. We point out that this same magnetoelectric effect could be present on other purely organic magnetic molecules [14,15].

ACKNOWLEDGMENTS

This work has been supported by the Argentinian agency CONICET, PICT 2012/1069 (A.V. and D.J.G.), and by the Brazilian agencies FAPEMIG, CAPES, and CNPq.

[1] N. A. Spaldin, MRS Bull. **42**, 385 (2017).
[2] N. A. Hill, J. Phys. Chem. B **104**, 6694 (2000).
[3] P. Jain, V. Ramachandran, R. J. Clark, H. D. Zhou, B. H. Toby, N. S. Dalal, H. W. Kroto, and A. K. Cheetham, J. Am. Chem. Soc. **131**, 13625 (2009).
[4] B. Kundys, A. Lappas, M. Viret, V. Kapustianyk, V. Rudyk, S. Semak, C. Simon, and I. Bakaimi, Phys. Rev. B **81**, 224434 (2010).
[5] J. Ding, H. Li, L. Wen, X. Kang, H. Li, and J. Zhang, J. Magn. Magn. Mater. **346**, 91 (2013).
[6] M. Fiebig, J. Phys. D: Appl. Phys. **38**, R123 (2005).
[7] N. A. Spaldin and M. Fiebig, Science **309**, 391 (2005).
[8] S. Thomas, S. Ramasesha, K. Hallberg, and D. García, Phys. Rev. B **86**, 180403(R) (2012).
[9] A. N. Aleshin, J. Y. Lee, S. W. Chu, J. S. Kim, and Y. W. Park, Appl. Phys. Lett. **84**, 5383 (2004).
[10] R. W. I. de Boer, T. M. Klapwijk, and A. F. Morpurgo, Appl. Phys. Lett. **83**, 4345 (2003).
[11] C. Goldmann, S. Haas, C. Krellner, K. P. Pernstich, D. J. Gundlach, and B. Batlogg, J. Appl. Phys. **96**, 2080 (2004).
[12] M. Watanabe, Y. J. Chang, S.-W. Liu, T.-H. Chao, K. Goto, I. Minarul, C.-H. Yuan, Y.-T. Tao, T. Shinmyozu, and T. J. Chow, Nat. Chem. **4**, 574 (2012).

[13] G. Giri, D. Dey, M. Kumar, S. Ramasesha, and Z. G. Soos, Phys. Rev. B **95**, 224408 (2017).
[14] M. Rano, S. K. Ghosh, and D. Ghosh, Chem. Sci. **10**, 9270 (2019).
[15] A. Valentim, G. A. Bocan, J. D. Fuhr, D. J. García, G. Giri, M. Kumar, and S. Ramasesha, Phys. Chem. Chem. Phys. **22**, 5882 (2020).
[16] M. Murai, S. Iba, H. Ota, and K. Takai, Org. Lett. **19**, 5585 (2017).
[17] L. Salem, *The Molecular Orbital Theory of Conjugated Systems* (W. A. Benjamin, New York, 1966).
[18] B. Purushothaman, M. Bruzek, S. Parkin, A. Miller, and J. Anthony, Angew. Chem. Int. Ed. **50**, 7013 (2011).
[19] C. Tönshoff and H. Bettinger, Angew. Chem., Int. Ed. **49**, 4125 (2010).
[20] D. I. Khomskii, *Basic Aspects of the Quantum Theory of Solids: Order and Elementary Excitations* (Cambridge University Press, New York, 2010).
[21] Z. Qu, S. Zhang, C. Liu, and J.-P. Malrieu, J. Chem. Phys. **134**, 021101 (2011).
[22] G. Chiappe, E. Louis, E. San-Fabin, and J. A. Vergs, J. Phys.: Condens. Matter **27**, 463001 (2015).
[23] N. Guihery, D. Maynau, and A. Jean-Paul Malrieu, New J. Chem. **22**, 281 (1998).
[24] A. A. Ovchinnikov, Theor. Chim. Acta **47**, 297 (1978).
[25] R. Pariser and R. G. Parr, J. Chem. Phys. **21**, 466 (1953).
[26] J. A. Pople, J. Chem. Soc. Faraday Trans. **49**, 1375 (1953).
[27] V. M. L. Durga Prasad Goli, S. Prodhan, S. Mazumdar, and S. Ramasesha, Phys. Rev. B **94**, 035139 (2016).
[28] S. Prodhan and S. Ramasesha, Phys. Rev. B **97**, 195125 (2018).
[29] M. Schüler, M. Rösner, T. O. Wehling, A. I. Lichtenstein, and M. I. Katsnelson, Phys. Rev. Lett. **111**, 036601 (2013).
[30] F. Lin and E. S. Sorensen, Phys. Rev. B **78**, 085435 (2008).
[31] B. Sinha, I. D. L. Albert, and S. Ramasesha, Phys. Rev. B **42**, 9088 (1990).
[32] Z. G. Soos, S. Ramasesha, and D. S. Galvão, Phys. Rev. Lett. **71**, 1609 (1993).
[33] Y. Anusooya, S. K. Pati, and S. Ramasesha, J. Chem. Phys. **106**, 10230 (1997).
[34] T. O. Wehling, E. Sasioglu, C. Friedrich, A. I. Lichtenstein, M. I. Katsnelson, and S. Blügel, Phys. Rev. Lett. **106**, 236805 (2011).
[35] P. Baettig, C. Ederer, and N. A. Spaldin, Phys. Rev. B **72**, 214105 (2005).
[36] J. Hubbard, Proc. R. Soc. London, Ser. A **276**, 238 (1963).
[37] S. R. White, Phys. Rev. Lett. **69**, 2863 (1992).
[38] I. Peschel, N. Kaulke, X. Q. Wang, and K. Hallberg, editors, *Density-Matrix Renormalization: A New Numerical Method in Physics, Lecture Notes in Physics*, Vol. 528 (Springer, Berlin, 1999).
[39] K. A. Hallberg, Adv. Phys. **55**, 477 (2006).
[40] E. Lieb and D. Matris, in *Condensed Matter Physics and Exactly Soluble Models: Selecta of Elliott H. Lieb*, edited by B. Nachtergaele, J. P. Solovej, and J. Yngvason (Springer, Berlin, 2004), p. 135.
[41] E. Lieb and D. Mattis, J. Math. Phys. **3**, 749 (1962).
[42] R. Arita, K. Kuroki, H. Aoki, A. Yajima, M. Tsukada, S. Watanabe, M. Ichimura, T. Onogi, and T. Hashizume, Phys. Rev. B **57**, R6854 (1998).
[43] K. Ohno, Theor. Chim. Acta **2**, 219 (1964).